

Opponent melanopsin and S-cone signals in the human pupillary light response

Manuel Spitschan^a, Sandeep Jain^b, David H. Brainard^{a,1}, and Geoffrey K. Aguirre^{b,1}

Departments of ^aPsychology and ^bNeurology, University of Pennsylvania, Philadelphia, PA 19104

Edited by Dennis M. Dacey, The University of Washington, Seattle, WA, and accepted by the Editorial Board September 12, 2014 (received for review January 17, 2014)

In the human, cone photoreceptors (L, M, and S) and the melanopsin-containing, intrinsically photosensitive retinal ganglion cells (ipRGCs) are active at daytime light intensities. Signals from cones are combined both additively and in opposition to create the perception of overall light and color. Similar mechanisms seem to be at work in the control of the pupil's response to light. Uncharacterized however, is the relative contribution of melanopsin and S cones, with their overlapping, short-wavelength spectral sensitivities. We measured the response of the human pupil to the separate stimulation of the cones and melanopsin at a range of temporal frequencies under photopic conditions. The S-cone and melanopsin photoreceptor channels were found to be low-pass, in contrast to a band-pass response of the pupil to L- and M-cone signals. An examination of the phase relationships of the evoked responses revealed that melanopsin signals add with signals from L and M cones but are opposed by signals from S cones in control of the pupil. The opposition of the S cones is revealed in a seemingly paradoxical dilation of the pupil to greater S-cone photon capture. This surprising result is explained by the neurophysiological properties of ipRGCs found in animal studies.

melanopsin | ipRGCs | pupillary light response | opponency

Under daylight conditions, human visual perception originates with signals generated by three classes of cone photoreceptors (the L, M, and S cones; Fig. 1A, Left) with peak sensitivities at long, middle, and short wavelengths of visible light (Fig. 1A, Center).

Distinct neural pathways process signals originating in cone photoreceptors for visual perception. Luminance pathways combine signals from separate classes of cones synergistically, providing a spectrally broadband indication of the overall light intensity at each location in the retinal image. Red–green and blue–yellow chromatic channels combine signals from separate classes of cones in an opponent (subtractive) fashion, providing sensitivity to the relative spectral content of light and supporting the perception of color independent of luminance (1).

A parallel set of pathways contributes to the response of the pupil of the eye to light. Most familiar is a synergistic cone effect that causes the pupil to constrict in response to increased luminance. Illustrating a commonality of principles that characterize neural mechanisms for perception and pupil response, rectified signals from red–green and blue–yellow opponent channels also contribute to the pupil's light response (2–7).

Recently, it has been discovered that mammalian retinas contain an additional photoreceptor class that also operates under daylight conditions. Intrinsically photosensitive retinal ganglion cells (ipRGCs) express the photopigment melanopsin, which has a peak spectral sensitivity (480 nm) between that of S and M cones (8, 9). Among other, “non-image-forming” functions of the eye, melanopsin-containing ipRGCs contribute to a delayed and sustained constriction of the pupil (10). Studies in patients with loss of photoreceptor function (11) suggest that melanopsin may also contribute to conscious visual perception.

The discovery of an additional photoreceptor class raises the fundamental question of how melanopsin signals are combined with those from the cones. Do melanopsin signals add to cones

to measure overall light intensity, or do they interact in an opponent fashion, enhancing the ability to detect changes in the relative spectrum of incident light?

Single-unit studies of the primate retina find that L- and M-cone signals add with those of melanopsin to produce the responses of ipRGCs but suggest that signals from S cones are inhibitory (12) (Fig. 1A, Right). Prior studies of short-wavelength light upon the human pupil response preceded the discovery of melanopsin and have offered complicated results. A transient constriction of the pupil was found to follow the offset of a short-wavelength stimulus on a long-wavelength background (2), and the results were interpreted in terms of an S-cone opponent input to the control of the pupil. However, alternation between short- and long-wavelength tritanopic metamers that yielded equivalent excitation of L and M cones was found to modulate the pupil in a manner suggesting in-phase S and L/M cone contributions to the pupillary light response (13). Critically, the interpretation of these earlier results—and particularly the relative contribution of the S cones and melanopsin to the pupil response—must be revisited given the overlapping spectral sensitivities of these two photoreceptor classes and the unknown role of melanopsin in mediating the earlier results.

Here we study how melanopsin and the three classes of cones contribute to the human pupillary light response (PLR). Despite the intuition that pupil size should be responsive to the overall intensity of the incident light, our results reveal that a spectrally opponent system involving melanopsin contributes to pupil control at photopic light levels. The nature of this response reflects,

Significance

Our eyes sense bright light using cones (L, M, and S) and recently discovered melanopsin-containing ganglion cells. Both S cones and melanopsin respond to blueish (short-wavelength) light. How does melanopsin interact with the cones in visual function? We measured the response of the human pupil to isolated stimulation of the different photoreceptors. Our work reveals a curious, opponent response to blue light in the otherwise familiar pupillary light response. Increased stimulation of S cones can cause the pupil to dilate, but this effect is usually masked by a stronger and opposite response from melanopsin-containing cells. Our results have clinical importance because the sensing of blue light is known to be related to seasonal depression, sleep, and pain from bright light.

Author contributions: M.S., D.H.B., and G.K.A. designed research; M.S., S.J., D.H.B., and G.K.A. performed research; M.S., S.J., D.H.B., and G.K.A. analyzed data; and M.S., D.H.B., and G.K.A. wrote the paper.

Conflict of interest statement: A patent on the alternative photoreceptor isolation method and its applications has been filed by the University of Pennsylvania with G.K.A., D.H.B., and M.S. as inventors.

This article is a PNAS Direct Submission. D.M.D. is a guest editor invited by the Editorial Board.

Freely available online through the PNAS open access option.

¹To whom correspondence may be addressed. Email: brainard@psych.upenn.edu or aguirreg@mail.med.upenn.edu.

This article contains supporting information online at www.pnas.org/lookup/suppl/doi:10.1073/pnas.1400942111/-DCSupplemental.

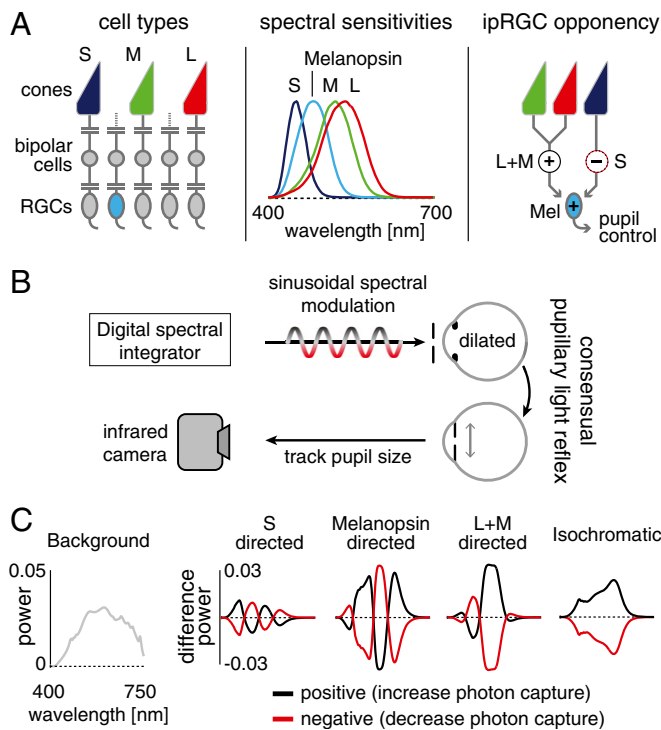


Fig. 1. Experimental design. (A, *Left*) L, M, and S cones and melanopsin-containing ipRGCs mediate vision at daytime light levels. (*Center*) Photoreceptor spectral sensitivities. (*Right*) Physiological measurements of ipRGCs find excitatory L and M cone inputs and inhibitory S-cone inputs (12). (B) A digital spectral integrator produces sinusoidal photoreceptor-directed modulations that pass through an artificial pupil into the pharmacologically dilated left eye. The consensual pupil response of the right eye is recorded. (C) Photoreceptor-directed modulations. Balanced changes in the spectrum of light around a background spectrum nominally isolate targeted photoreceptors.

qualitatively, the spectral opponency seen in ipRGCs: Signals from melanopsin combine additively with those from L and M cones and are opposed by signals from S cones.

Results

Using an infrared camera, we measured the consensual PLR of human participants while they observed sinusoidal modulations in the spectrum of a light (Fig. 1B). The stimulus modulations were designed to target specific photoreceptors. The cones and melanopsin have different but overlapping spectral sensitivities. Despite the overlap, it is possible to create sets of light spectra such that the absorption of photons is constant for all of the photoreceptor classes except one (14–16) (Fig. 1C). Modulation between a pair of these “silent substitution” spectra increases and decreases the response of (for example) melanopsin-containing ipRGCs while maintaining nominally constant stimulation of the cones. Separate modulations were designed for melanopsin, S cones, and L+M cones together (a modulation that varied luminance as well as chromaticity). An isochromatic modulation (melanopsin+S+M+L) was also used. All modulations were designed to produce 50% contrast on their targeted photoreceptor(s). Rods were silenced by modulating the spectra about a photopic background (~800 cd/m²). The stimulus was wide-field (27.5°), spatially uniform, and had the central 5° obscured to avoid variation in photoreceptor spectral sensitivity across the visual field caused by the presence of the foveal macular pigment (17). Simulations and control experiments support the specificity of the photoreceptor isolation (Figs. S1–S5 and Table S1).

We measured pupil responses from 16 subjects while they observed the different photoreceptor-directed modulations at two

flicker rates (0.05 and 0.5 Hz). The effect of the stimulation is apparent as a sinusoidal oscillation at the stimulation frequency in the raw traces of pupil response from one subject (Fig. 2A). Measurable pupil responses at the second harmonic of the stimulation frequency were also observed (Fig. S6). Because the mean pupil diameter was equivalent across photoreceptor stimulation directions and frequencies (Fig. S7) the pupil response can be expressed as a percent change.

The average response across cycles of the modulation at the stimulus frequency (Fig. 2B) reveals in both individuals and the group data that the L+M- and melanopsin-directed modulations produce pupil responses of similar phase. The S-cone modulation, however, produced responses with markedly different phase.

The relations between the different photoreceptor-driven responses are more easily apprehended on a polar plot (Fig. 3). Retinal ganglion cell electrophysiology suggests that melanopsin and L+M signals combine additively (12). We examined the relative amplitude and phase response for each subject to L+M and melanopsin modulations at the two frequencies (Fig. 3A). For each subject and temporal frequency these responses are expressed relative to the complex sum of responses across the L+M, melanopsin, and S photoreceptor directions for that subject (which approximates the pupil response to an isochromatic modulation; Fig. S8). This normalization removes from the data individual differences in an overall delay between stimulus onset and pupil response common to all photoreceptors.

At high temporal frequency (0.5 Hz), the melanopsin- and L+M-evoked pupillary responses are in phase (Fig. 3A, *Upper*). At the lower frequency (0.05 Hz), L+M- and melanopsin-evoked responses become desynchronized in quadrature phase (Fig. 3B, *Lower*); this phase effect is examined further below.

Electrophysiology studies suggests that the S-cone inputs to ipRGCs are opponent to the melanopsin and luminance signals (12, 18). We examined the relationship between S-cone-driven pupil responses and a putative “pupil brightness” channel, constructed as the complex sum of the melanopsin- and L+M-cone-driven responses. Across subjects, the S cones produced an antiphase,

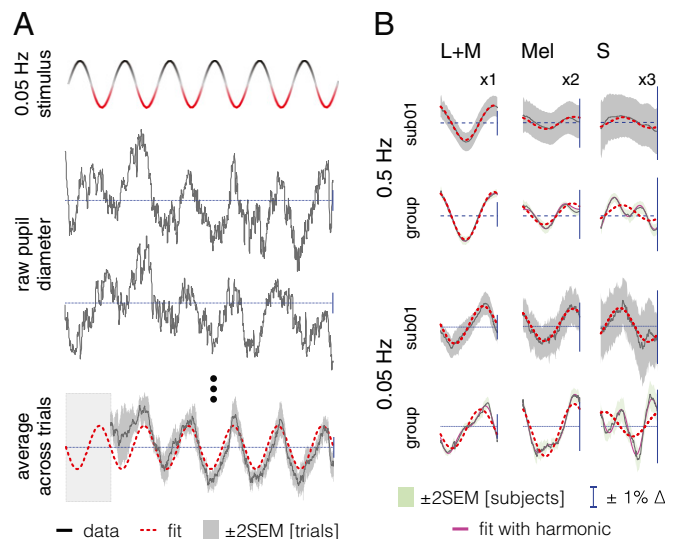


Fig. 2. S input to the PLR is opponent to L+M and melanopsin. (A, *Top*) Stimulus modulation over time between positive and negative spectra. (*Middle*) Pupil traces for two 120-s trials (sub01, 0.05 Hz, L+M). (*Bottom*) Average data (12 trials; same subject/condition; first 20 s discarded) fit with a sinusoid at the stimulus fundamental. (B) One cycle of the PLR [sub01 and group average over 16 subjects (black lines); melanopsin responses $\times 2$ scale, S responses $\times 3$]. Red dashed lines show fit with fundamental. Where visible, magenta lines are the fits with fundamental and second harmonic.

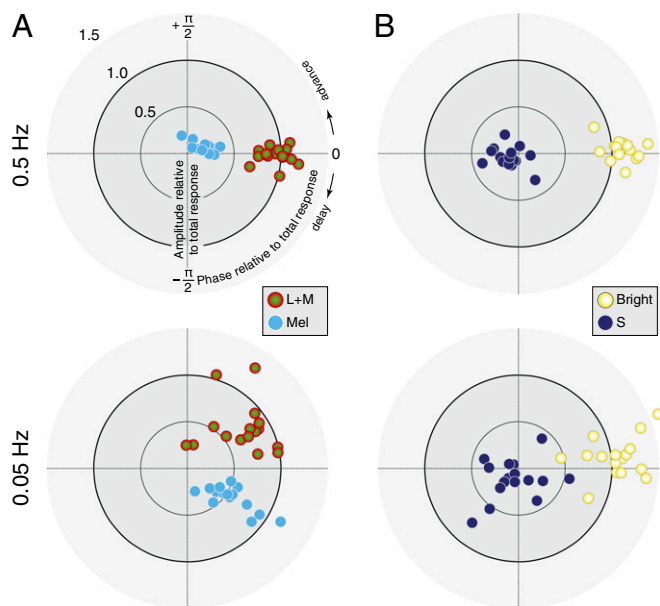


Fig. 3. PLR phase reveals synergy and opponency. (A, Upper) L+M and melanopsin responses are in phase at 0.5 Hz. Each point shows data for one subject. (Lower) L+M and melanopsin responses are in quadrature phase at 0.05 Hz. (B) For most subjects, S responses are opponent to the complex sum of L+M and melanopsin (pupil brightness) at both 0.5 Hz and 0.05 Hz. In all plots, amplitude and phase for each subject are shown relative to the complex sum of L+M, melanopsin, and S responses for that subject/temporal frequency.

steady-state pupil response at 0.5 and 0.05 Hz relative to the pupil brightness-driven response (Fig. 3B).

Despite the generally antiphase relationship of S-cone responses across subjects, there were individual differences in the phase effects greater than individual measurement error (Table S2). Additionally, we wished to understand the origin of the quadrature phase desynchronization between melanopsin- and L+M-driven pupil responses at lower frequencies. We studied two subjects in greater depth, measuring pupil responses to the photoreceptor-directed modulations at six temporal frequencies between 0.01 and 2 Hz. Fig. 4A presents the amplitude responses across temporal frequencies for both subjects. These transfer functions characterize the temporal filtering properties of each photoreceptor channel. The pupil response mediated by the L+M cone pathway was band-pass, with a maximum response at 0.1 Hz, rolling off for higher frequencies. The responses to melanopsin and S-cone stimulation were low-pass, maximal at the lowest measured modulation frequency (0.01 Hz), and markedly reduced by 0.5 Hz.

Fig. 4B presents the phase of the response across frequencies of stimulation. We modeled simultaneously the amplitude and phase data with a time-invariant, linear model composed of a “fast” and “slow” temporal filter (19). The amplitude and phase data were well fit by the model, including a fixed temporal delay in both observers across photoreceptor channels of ~250 ms and a negative amplitude response to S-cone modulation for the fast filter (Table S2). The separate filter properties for L+M and melanopsin account for the quadrature phase desynchronization of these responses at lower temporal frequencies. Further, differences in model parameters account for the finding in subject 02 of an S-cone response that seems in-phase with L+M and melanopsin responses at low frequencies, despite having an S-cone opponent input to the fast filter of the model PLR. This individual difference arises, at least in part, because the slow filter S-cone component is of the same sign as the melanopsin component of the response for this subject.

We then applied this model to the group data. We obtained the average amplitude and phase of response across the 16 subjects

for each combination of photoreceptor target and modulation frequency. The two-filter model fits the average amplitude and phase data (Fig. 5A) with parameters similar to those found for subject 01 (Table S2). When expressed as a polar plot (Fig. 5B), the agreement between the group data and model fits is apparent. Interestingly, there is systematic “rotation” of the phase of both the pupil brightness and S-cone responses at the lower temporal frequency that is not captured by the model. This may result from individual differences in the phase of S-cone responses at low temporal frequencies, as is seen between subject 01 and subject 02 (Fig. 4), because the average data do not fully constrain the model and the fits shown are based on parameters obtained for subject 01.

Discussion

We examine how signals originating in the melanopsin ipRGCs combine with signals from cones to regulate the size of the human pupil under daylight conditions. Although it is intuitive that the pupil should contract when more light stimulates any of these photoreceptors, we find instead that signals from L+M cones and melanopsin are opposed by signals from S cones in the PLR.

This result, although counterintuitive for the pupil, is consistent with the cellular properties of the ipRGCs. Giant ipRGCs receive inhibitory input from S cones (12), but it is not immediately clear which synaptic inputs mediate this S-off sensitivity (20). Because there is presently no evidence for an S-off bipolar cell in the primate retina (20), the opponent pupil response we observe to S-cone stimulation seems likely explained by the negative S-cone input to ipRGCs.

Our finding of antagonistic effects of short-wavelength light upon the human pupil response helps clarify prior results. In

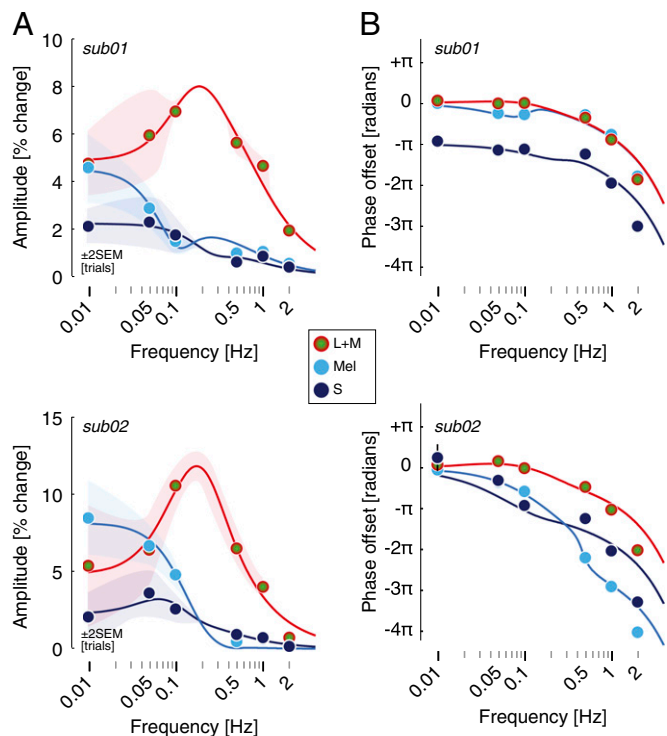


Fig. 4. A two-component linear filter model accounts for the photoreceptor-specific temporal transfer functions of the PLR via S-cone opponency. (A) Amplitude of the PLR fundamental for three photoreceptor-directed modulations from two subjects. Points show data and solid lines show the fit of the linear filter model. The sign of the S input to the fast component of the model is negative relative to the sign of the L+M and melanopsin input. (B) Phase of the PLR fundamental of the pupil as a function of stimulus temporal frequency. Error bars are generally smaller than plot symbols.

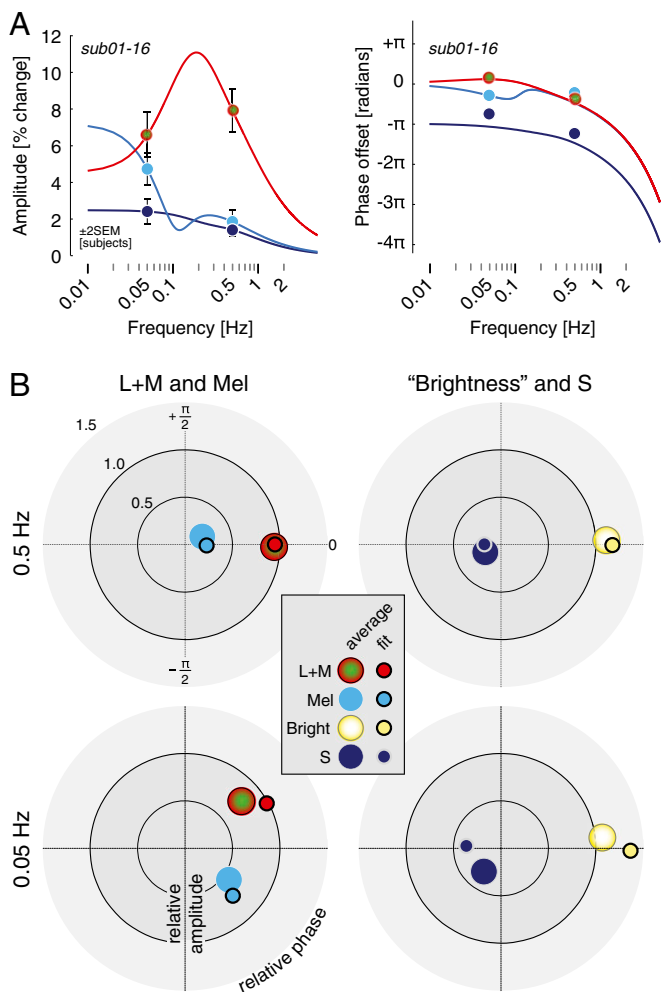


Fig. 5. Group PLR data are well fit by the two component linear filter model. (A) The mean response across all subjects (01–16) is shown at 0.05 and 0.5 Hz, for L+M-, melanopsin-, and S-cone-directed modulations. Fit values are derived from those found for subject 01, with only amplitude parameters adjusted (Table S2). This is because the average data are available at only two temporal frequencies and do not sufficiently constrain all parameters of the model. To obtain the average data plotted, amplitudes and phases were averaged separately (i.e., average amplitude obtained without consideration of phase, average phase obtained without consideration of amplitude). The model was fit to the data as plotted. (B) Polar-plot representations of the group data with model fit points, following conventions as in Fig. 3. The data are normalized separately for each temporal frequency. Error bars (± 2 SEM across subjects) are smaller than the plot points for the data.

a previous study, weak short-wavelength contributions relative to L and M cones were observed variably across observers (13). The weak nature of the responses they found may result from opposed S and melanopsin stimulation. Another study examined the transient, miotic pupil off response to cessation of a temporally extended light pulse (2). This constrictive off response was observed under all wavelength conditions, but the size of the constriction was found to decrease with increasing peak wavelength of the monochromatic light used in the study. The authors observed that the shape of the short-wavelength lobe of the transient off response changed with stimulus amplitude, which they interpreted as a “failure of univariance” and consistent with the existence of an additional, then unknown, photopigment (2). The opposed S-cone- and melanopsin-driven pupillary responses we find helps explain this result.

Despite the opponent S-cone effect, a paradoxical dilation of the pupil in response to a narrow-band blue light stimulus is not

seen under physiologic conditions. It seems this is because the constrictive effect of melanopsin stimulation overwhelms the smaller S-cone-driven responses. Interestingly, a transient, paradoxical constriction of the pupil when switching to darkness from bright light is a feature of several human retinal disorders (21), raising the possibility that relative disruption of photoreceptor classes can reveal the opponency inherent in the PLR.

In agreement with prior work (22), we find that melanopsin provides an ever-greater input to pupil control at ever-longer time scales, reaching a plateau at our lowest studied frequency of 0.01 Hz. This is consistent with a long time scale of integration of melanopsin signals (9, 12, 23). At higher frequencies the melanopsin contribution to the pupil is markedly attenuated, falling to a fractional component above 0.5 Hz. The small response that remains at higher temporal frequencies could derive from imperfections in our stimulus precision. We calculate that our nominally melanopsin-isolating stimulus might produce $\sim 4\%$ of residual stimulation of L and M cones, respectively (Fig. S2 and Table S1; this residual stimulation was $\sim 2\%$ in control experiments with further stimulus refinements, Fig. S5). Although this small degree of stimulus “splatter” cannot account for the robust melanopsin-driven response observed at low temporal frequencies (where it matches and exceeds L+M-driven responses) it could contribute to the small response that remains above 0.5 Hz.

There have been several prior studies of the pupil temporal transfer function using either broadband spectral modulation (24–31) or monochromatic light (32, 33). A low-pass pupil response with maximal amplitude at the lowest measured modulation frequency is generally found (Fig. S9), as is the case for our isochromatic modulation (Fig. S8). This overall response combines the contributions of the individual photoreceptors, shown here to be low-pass for S-cone- and melanopsin-driven modulation and band-pass (peaking at 0.1 Hz) for L+M-driven modulation. A band-pass response to cone (L+M+S), rod, and combined cone-rod-directed modulations was also recently reported (34) under mesopic conditions (≤ 1 cd/m²), and a faster peak response (1 Hz) was found compared with the current work. This may be related to the marked difference in luminance and contrast regimes between this prior work compared with our study (26).

We found that the amplitude and phase responses of the pupil to differential photoreceptor stimulation were well fit with a linear model of temporal filters. There were, however, systematic aspects of our data not fit by the model. Second harmonic (frequency doubled) pupil responses were observed to each of the photoreceptor-directed stimulations (Fig. S6). These harmonic responses are indicative of a nonlinearity in the pupil response and have been reported previously in response to sinusoidal light flux (28). Our data cannot locate the stage of the nonlinearity between the retina and pupillary muscles (including in subcortical or cortical pathways). Also, systematic differences were observed between individuals in the phase of S-cone-driven responses relative to L+M+melanopsin-driven responses at low temporal frequencies. We regard the model as a useful tool for capturing the systematic properties of the data, relating individual results to average group effects and demonstrating the extent of the integrated pupil response that may be explained by linear summation of its photoreceptor components. We do not, however, have a strong stance regarding its plausible implementation in biological systems. Clearly, there is additional information in the photoreceptor-specific temporal responses at both the group and individual level to be characterized and related to the neurophysiology of the visual pathway.

Could the synergistic and opponent pupil responses we find also be reflected in perception? Similar to our findings in the pupil response, there is evidence of S-cone opponency in the perception of the luminance of stimuli (35, 36). In the pupil response, we find that S-cone signals oppose the sum of melanopsin and L+M signals, which we term here pupil “brightness.”

Melanopsin may combine with L+M signals in perception as well to provide an overall sense of image brightness. Evidence for this synergy has been reported in mice and humans (37). Our results suggest that the intimate relationship between visual perception and pupil control may continue to hold even as novel photopigments and opponency expand our understanding of the retina.

Methods

Cone spectral sensitivities for construction of photoreceptor-directed modulations (Dataset S1) were taken from tabular values (17), and in the case of melanopsin by shifting the Stockman–Sharpe nomogram to have peak spectral sensitivity at $\lambda_{\max} = 480$ nm. Prereceptor filtering of melanopsin was assumed to match that of cones, and we assumed a peak optical density for melanopsin of 0.3.

Observers viewed the sinusoidal spectral modulations in peripheral stimulation with a field diameter of 27.5°. The central 5° diameter of visual angle was obscured and a hairline vertical, horizontal, and annular grid was visible. Pupillary responses were recorded using an infrared eye tracker (Cambridge Research Systems) sampling at 50 Hz.

Two primary observers (sub01 and 02, authors G.K.A. and S.J.) viewed the four modulation directions at 0.01, 0.05, 0.1, 0.5, 1, and 2 Hz in trials of 120 s each. An additional 14 observers viewed the L+M-, melanopsin-, and S-directed stimulation at 0.05 and 0.5 Hz during 45-s trials. Four other observers were recruited for the

study but excluded from the protocol because of poor eye tracking owing to epicanthal folds or an inability to suppress blinking. All stimuli were presented in counterbalanced sequence. Stimulus onset was windowed by a 3-s half-cosine and stimulus phase was randomized for subs 03–16. A 5-min adaptation to the background preceded each data collection session, and the subject remained exposed to the background between trials.

Responses were averaged across trials. The first 20 or 5 s (for the 120- and 45-s trials, respectively) of each trial were discarded before fitting to allow measurement of the steady-state pupil response. Response amplitude (in percent change units; Fig. S7) and phase were obtained by least-squares fitting of a sine and cosine to the average response (Dataset S2). Noise measures were obtained by similar fitting to the residuals of the data and analyzing responses at nonstimulated temporal frequencies (Fig. S10). We did not correct the data for stimulus-locked noise, but the effect of such corrections would be small (Fig. S10).

Detailed methods are described in *SI Methods*.

ACKNOWLEDGMENTS. We thank Sakibul Alam, Christopher Broussard, Nicolas Cottaris, and Fred Letterio for technical assistance. Long Luu assisted with implementation of the linear filter model. This work was supported by National Institutes of Health Grants R01 EY020516 (to G.K.A.), R01 EY10016 (to D.H.B.), and P30 EY001583 (Core Grant for Vision Research) and Deutscher Akademischer Austauschdienst (M.S.).

1. Stockman A, Brainard DH (2010) Color vision mechanisms. *OSA Handbook of Optics*, ed Bass M (McGraw-Hill, New York), pp 11.11–11.104.
2. Kimura E, Young RS (1999) S-cone contribution to pupillary responses evoked by chromatic flash offset. *Vision Res* 39(6):1189–1197.
3. Kimura E, Young RS (2010) Sustained pupillary constrictions mediated by an L- and M-cone opponent process. *Vision Res* 50(5):489–496.
4. Kimura E, Young RS (1996) A chromatic-cancellation property of human pupillary responses. *Vision Res* 36(11):1543–1550.
5. Krastel H, Alexandridis E, Gertz J (1985) Pupil increment thresholds are influenced by color opponent mechanisms. *Ophthalmologica* 191(1):35–38.
6. Tsujimura S, Wolffsohn JS, Gilmartin B (2001) A linear chromatic mechanism drives the pupillary response. *Proc Biol Sci* 268(1482):2203–2209.
7. Young RS, Alpern M (1980) Pupil responses to foveal exchange of monochromatic lights. *J Opt Soc Am* 70(6):697–706.
8. Provencio I, et al. (2000) A novel human opsin in the inner retina. *J Neurosci* 20(2):600–605.
9. Berson DM, Dunn FA, Takao M (2002) Phototransduction by retinal ganglion cells that set the circadian clock. *Science* 295(5557):1070–1073.
10. Gamlin PD, et al. (2007) Human and macaque pupil responses driven by melanopsin-containing retinal ganglion cells. *Vision Res* 47(7):946–954.
11. Zaidi FH, et al. (2007) Short-wavelength light sensitivity of circadian, pupillary, and visual awareness in humans lacking an outer retina. *Curr Biol* 17(24):2122–2128.
12. Dacey DM, et al. (2005) Melanopsin-expressing ganglion cells in primate retina signal colour and irradiance and project to the LGN. *Nature* 433(7027):749–754.
13. Verdon W, Howarth PA (1988) The pupil's response to short wavelength cone stimulation. *Vision Res* 28(10):1119–1128.
14. Donner KO, Rushton WA (1959) Retinal stimulation by light substitution. *J Physiol* 149:288–302.
15. Estévez O, Spekrijse H (1982) The “silent substitution” method in visual research. *Vision Res* 22(6):681–691.
16. Tsujimura S, Ukai K, Ohama D, Nuruqi A, Yunokuchi K (2010) Contribution of human melanopsin retinal ganglion cells to steady-state pupil responses. *Proc Biol Sci* 277(1693):2485–2492.
17. CIE (2006) Fundamental chromaticity diagram with physiological axes – Part 1. Technical Report 170-1 (Central Bureau of the Commission Internationale de l'Éclairage, Vienna).
18. Allen AE, Brown TM, Lucas RJ (2011) A distinct contribution of short-wavelength-sensitive cones to light-evoked activity in the mouse pretectal olivary nucleus. *J Neurosci* 31(46):16833–16843.
19. Watson AB (1986) Temporal sensitivity. *Handbook of Perception and Human Performance*, eds Boff K, Kaufman L, Thomas J (Wiley, New York), Vol 1, pp 6.1–6.43.
20. Dacey DM, Crook JD, Packer OS (2014) Distinct synaptic mechanisms create parallel S-ON and S-OFF color opponent pathways in the primate retina. *Vis Neurosci* 31(2):139–151.
21. Frank JW, Kushner BJ, France TD (1988) Paradoxical pupillary phenomena. A review of patients with pupillary constriction to darkness. *Arch Ophthalmol* 106(11):1564–1566.
22. Gooley JJ, et al. (2012) Melanopsin and rod-cone photoreceptors play different roles in mediating pupillary light responses during exposure to continuous light in humans. *J Neurosci* 32(41):14242–14253.
23. Do MT, et al. (2009) Photon capture and signalling by melanopsin retinal ganglion cells. *Nature* 457(7227):281–287.
24. Bleichert A (1957) Die Lichtreaktion der Pupille als Regelvorgang. *Albrecht Von Graefes Arch Ophthalmol* 159(4):396–410.
25. Hornung J, Stegemann J (1964) *Ein nichtlineares kybernetisches Modell für die Pupillenreaktion auf Licht* (Westdeutscher, Köln, Germany).
26. Sandberg A, Stark L (1968) Wiener G-function analysis as an approach to non-linear characteristics of human pupil light reflex. *Brain Res* 11(1):194–211.
27. Stark L, Baker F (1959) Stability and oscillations in a neurological servomechanism. *J Neurophysiol* 22(2):156–164.
28. Sherman PM, Stark L (1957) A servoanalytic study of consensual pupil reflex to light. *J Neurophysiol* 20(1):17–26.
29. Stegemann J (1957) Über den Einfluß sinusförmiger Leuchtdichteänderungen auf die Pupillenweite. *Pflugers Arch Gesamte Physiol Menschen Tiere* 264(2):113–122.
30. Varjú D (1967) Nervöse Wechselwirkung in der pupillomotorischen Bahn des Menschen. I. Unterschiede in den Pupillenreaktionen auf monoculare und binoculare Lichtreize. *Kybernetik* 3(5):203–214.
31. van der Wildt GJ, Bouman MA (1974) Dependence of the dynamic behaviour of the human pupil system on the input signal. *Opt Acta (Lond)* 21(1):59–74.
32. Clarke RJ, Zhang H, Gamlin PD (2003) Characteristics of the pupillary light reflex in the alert rhesus monkey. *J Neurophysiol* 89(6):3179–3189.
33. Zangemeister WH, Gronow T, Grzyska U (2009) Pupillary responses to single and sinusoidal light stimuli in diabetic patients. *Neural Int* 1(1):e19.
34. Barrionuevo PA, et al. (2014) Assessing rod, cone, and melanopsin contributions to human pupil flicker responses. *Invest Ophthalmol Vis Sci* 55(2):719–727.
35. Lee J, Stromeyer CF, 3rd (1989) Contribution of human short-wave cones to luminance and motion detection. *J Physiol* 413:563–593.
36. Stockman A, MacLeod DI, DePriest DD (1991) The temporal properties of the human short-wave photoreceptors and their associated pathways. *Vision Res* 31(2):189–208.
37. Brown TM, et al. (2012) Melanopsin-based brightness discrimination in mice and humans. *Curr Biol* 22(12):1134–1141.